

350 GHz NbN HOT ELECTRON BOLOMETER MIXER

by

H.Ekström^{a)}, B.Karasik^{b)}, E.Kollberg^{a)}, G.Gol'tsman^{b)}, and E.Gershenzon^{b)}

^{a)}Department of Microwave Technology, Chalmers University of Technology, S-41296 Göteborg, Sweden

^{b)}Department of Physics, Moscow State Pedagogical University, Moscow 119435, Russia

ABSTRACT

Superconducting NbN hot-electron bolometer (HEB) mixer devices have been fabricated and measured at 350 GHz. The HEB is integrated with a double dipole antenna on an extended crystalline quartz hyper hemispherical substrate lens. Heterodyne measurement gave a -3 dB bandwidth, mainly determined by the electron-phonon interaction time, of about 680 and 1000 MHz for two different films with $T_c = 8.5$ and 11 K respectively. The measured DSB receiver noise temperature is around 3000 K at 800 MHz IF frequency. The main contribution to the output noise from the device is due to electron temperature fluctuations with the equivalent output noise temperature $T_{FL} \approx 100$ K. T_{FL} has the same frequency dependence as the IF response. The contribution from Johnson noise is of the order of T_c . The RF coupling loss is estimated to be ≈ 6 dB. The film with lower T_c , had an estimated intrinsic low-frequency conversion loss ≈ 7 dB, while the other film had a conversion loss as high as 14 dB. The difference in intrinsic conversion loss is explained by less uniform absorption of radiation. Measurements of the small signal impedance shows a transition of the output impedance from the DC differential resistance $R_d = dV/dI$ in the low frequency limit to the DC resistance $R_0 = U_0/I_0$ in the bias point for frequencies above 3 GHz. We judge that the optimum shape of the IV-characteristic is more easily obtained at THz frequencies where the main restriction in performance should come from problems with the RF coupling.

INTRODUCTION

There is a continuous need of improved heterodyne receivers for radio astronomy at terahertz frequencies. Mainly one type mixer device is currently in use at and above 1 THz, namely the Schottky diode mixer [1]. The sensitivity is however lower than what is required for several planned projects. The low noise InSb hot-electron bolometer mixers, used up to about 800 GHz [2], have an IF bandwidth of about 2 MHz, which is too narrow for many applications. Nb trilayer SIS quasi-particle tunnel junctions [3] are very sensitive mixer devices, but so far only for frequencies below the energy gap of Nb (≈ 700 GHz). There are however different types of new promising hot-electron bolometric devices under development; 2DEG devices using the temperature dependent mobility of a 2-dimensional electron gas [4], and superconducting hot electron bolometers (HEB) utilizing the electron temperature dependent resistance in superconducting narrow thin film strips [5-7]. The mixer performance of the Nb HEB mixer at 20 GHz is promising [6], however the bandwidth of Nb devices, determined by the electron-phonon interaction time, τ_{e-ph} , is narrow (≈ 90 MHz). An improved bandwidth of Nb mixers is obtained in very short devices [8]. The response or hot electron temperature relaxation time is reduced when the electron diffusion time out from the device is shorter than the electron-phonon interaction time. A bandwidth of about 2 GHz has been measured [7] in this type of device. It is also possible to obtain a larger bandwidth with materials with shorter τ_{e-ph} . We show here that it is possible to have a bandwidth larger than 1 GHz with NbN devices. NbN has a larger energy gap than Nb, why a larger signal frequency is required to get uniform absorption in the film at low temperatures, which is required for optimum mixer performance. At THz frequencies this is fulfilled, i.e. the energy gap $\Delta_{NbN}(T) < h\nu/2$. However, for the current measurements at 350 GHz, the device has to be heated up to within 1 K below T_c to obtain $\Delta < h\nu/2$. For the heated sample, measured noise, conversion gain and impedance agrees reasonably well with theory. Improved agreement is expected at higher signal frequencies.

THE NbN HEB DEVICE

The HEB devices are made of NbN films, either 100 or 200 Å thick. The films are patterned to form 11 parallel, 1.5 μm wide and 5 μm long strips. The devices are integrated with double dipole antennas [9] on extended hemispherical crystalline-quartz substrate lenses [10]. The NbN-films are DC magnetron sputtered [11] on non-heated substrates and patterned by conventional photo-lithography and plasma etching (30 sccm He + 10 sccm CF₄ (incl. 8% O₂)). The antenna and contacts are made of 3000 Å Nb + a 1500 Å thick layer of Au, patterned by lift-off. We have tested two film of different

quality. Devices made from the first 200 Å thick film, represented by the typical device #A, has lower T_C , critical current I_C , unpumped resistive state current I_{00} , and surface resistance R_s , than device #B, made from a much thinner (≈ 100 Å) film of higher quality, see table I. However, together with the improved I_{00} and T_C , is a degradation of the superconducting transition width ΔT_C , see Fig. 1. This figure also shows that device #B has a foot structure in the $R(T)$ curve. Future devices will be made on Si substrates with contacts made of ≈ 3000 Å thick Au without the additional Nb layer. This will improve the film quality with respect to transition width, and prevent possible degradation by Andreev reflections [12] in the NbN-Nb interface, which could be important if the devices are made much shorter .

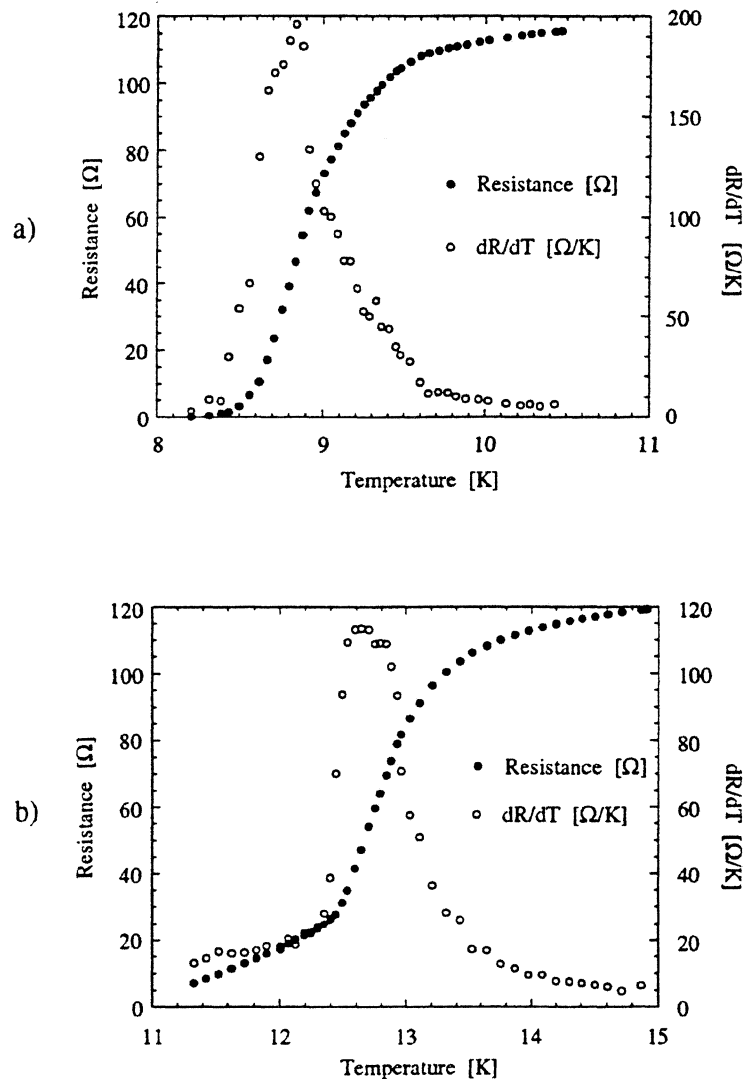


Fig. 1. Plot a) shows $R(T)$ and dR/dT for device #A, and plot b) shows the same for device #B.

TABLE I

#	d [Å]	R _s ¹⁾ [Ω]	R _N ¹⁾ [Ω]	dR/dT [Ω/K]	T _c ²⁾ [K]	T _c ³⁾ [K]	ΔT _c [K]	I _c [μA]	I _∞ [μA]
A	200	390	122	190	8.5	8.8	0.5	1900	600
B	100	500	150	110	11	12.6	1 ⁴⁾	3150	1130

¹⁾ At room temperature

²⁾ At onset of resistance

³⁾ At maximum dR/dT

⁴⁾ Excluding the foot structure.

MEASUREMENT SET-UP

The measurements are made with the mixer mounted in a LHe cooled vacuum cryostat. Attached to the mixer mount are a resistive heater and a thermometer for temperature control. Signal and LO are combined with a 50 μm thick Mylar beamsplitter and fed to the mixer through a Teflon window and Fluorogold IR shield in the cryostat wall. The LO source is a 310-370 GHz BWO (Carcinotron), and the signal is obtained from a SBV quintupler pumped by a 70 GHz Gunn oscillator. Bandwidth and output noise measurements are made with a wideband (0.02-4 GHz) room temperature IF amplifier, while for mixer noise measurements a cooled 680 to 920 MHz balanced low noise amplifier¹ together with a cooled bias²-T are included in the IF chain. The output IF signal is registered on a spectrum analyser. Alignment of the set-up was done with the device in detection mode. The LO path was adjusted to obtain maximum reduction of bias current, while the signal path was adjusted using a lock-in amplifier to observe the response to the low-frequency modulated signal.

We have estimated the losses on the RF-side to be roughly about 5-7 dB. See Table II.

TABLE II

	loss [dB]
Mylar beamsplitter	1
Teflon window	0.5
Fluorogold IR shield	1
Quartz lens	2
Back lobe	1
Beam coupling	0.5
TOTAL loss	≈ 6 dB

¹ Supplied by R.Brady, NRAO; Noise temperature ≈6 K and ≈17 dB gain at 14 K.

² Radiall R44353533000-9437 bias-T, 0.1-1.5 GHz

BIAS POINTS

Fig. 2 shows typical IV-characteristics for the device with optimum bias points. Depending on the physical temperature of the device and frequency of the IF output signal, it is possible to find different optimum bias points. For low temperatures the IV-characteristic has a hysteretic behaviour with a critical current $I_c \neq 0$. In this case, for output frequencies not too far above the IF bandwidth the optimum bias point is found just beside the unstable region at the transition from the resistive state to the superconducting state. At these low temperatures and relatively large DC-powers, it is reasonable to believe that resistive domains are responsible for the resistive state, where also the main part of radiation is absorbed.

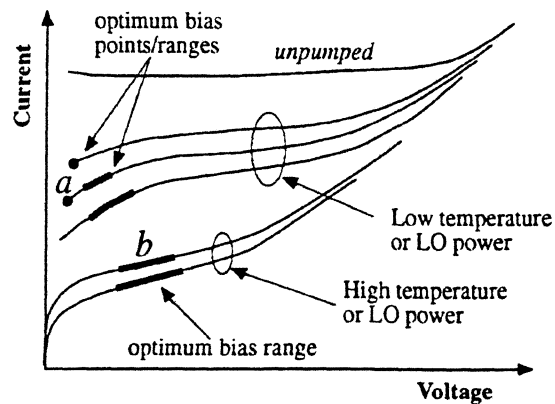


Fig. 2. Schematic of the optimum bias points and ranges for different temperatures and LO-powers for device #A. *a* shows the optimum bias point for low f_{IF} at low temperatures, and *b* shows the optimum bias range at high temperatures. This difference is probably valid only as long as the signal frequency ν at low temperatures is less than $2\Delta/h$. For higher ν the conversion should not be improved by an increased temperature (reduced Δ) for f_{IF} close to the IF bandwidth.

For IF frequencies a few times the IF bandwidth a shift of the optimum bias is observed. The optimum no longer found in "one point" for the lowest bias voltages, but there is instead an optimum bias-range at higher voltages (Fig. 2). For higher temperatures, when the supercurrent is suppressed, $I_c = 0$, the same kind of shift in optimum bias is found. At these higher temperatures the energy gap is reduced, and the radiation can be more uniformly absorbed over the whole film. A shift of optimum bias can also be found when the superconductivity is suppressed by increased LO-power instead of thermal heating. Moreover, for a certain range of temperatures or LO power, it is possible to find two optimum biases, one point just at the instability and one wide region for higher bias.

We believe there are two different mixing modes at high and low temperatures, i.e. at the bias point close to the instability and in regions of higher bias. We have also seen that the mixing mechanism dominating for larger bias has a wider bandwidth. A possible explanation is that at higher temperatures the resistive state is most likely due to vortex flow (more uniform), while at lower temperatures a slow motion of the domain walls contributes to the signal at low f_{IF} .

MIXER CONVERSION AND BANDWIDTH

The mixer conversion gain is given by Eq. 1 [6, 13].

$$G = 2(C_o I_o)^2 \frac{\chi^2 P_{LO} R_L}{(R_L + R_o)^2} \left(1 - C_o I_o^2 \frac{R_L - R_o}{R_L + R_o}\right)^{-2} \left(1 + (\omega \tau_{mix})^2\right)^{-1} \quad (1)$$

where χP_{LO} , R_L , R_o is the absorbed LO-power, load resistance, and bolometer DC-resistance respectively, and

$$C = C_o I_o^2 = \frac{dR}{dP} I_o^2 = \frac{dR}{d\theta} \frac{I_o^2}{G_e} = \frac{R_d - R_o}{R_d + R_o} \quad (2)$$

C is sometimes called the self-heating parameter, θ is the electron temperature, G_e the thermal conductivity between the electron system and the lattice, and R_d the DC differential resistance. Since the response of the HEB as bolometer is the same to DC and RF-power, these two can be compared in the IV-characteristic, and an estimation of the absorbed LO power and conversion gain can be made [6].

The two HEB devices described above have been compared in heterodyne measurements at 350 GHz. The IF bandwidth of device #B, with a larger T_c , shows an improved bandwidth (1000 MHz) compared to #A (680 MHz) (Fig. 3 and 4). This agrees qualitatively with the experimental data on the temperature dependence of the electron-phonon relaxation time [14] since

$$\text{Bandwidth}^{-1} = 2\pi\tau_{mix} \propto \tau_{e-ph} \propto \theta^{-1.6} \approx T_c^{-1.6} \quad (3)$$

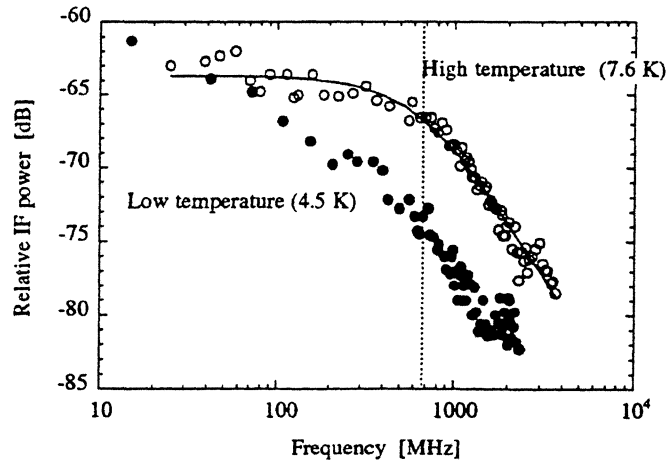


Fig. 3. IF response of sample #A at 4.5 K and 7.6 K.

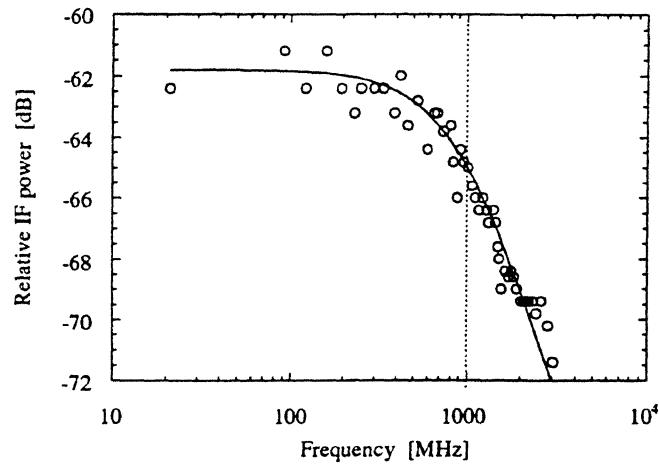


Fig. 4. IF response of sample #B at 11.6 K.

According to Eq. 1 and 2, a film of higher quality with a narrower transition width ΔT_c , i.e. larger $dR/d\theta$ at T_c , should have better conversion gain since it will give a larger self-heating parameter C . Device #A had an intrinsic conversion gain of -7 to -8 dB, estimated by Eq. (1), with an optimum absorbed LO power of $2 \mu\text{W}$, while the conversion gain of device #B (with larger I_c) was estimated to be -14 dB with an optimum absorbed LO power of $15 \mu\text{W}$. In both cases the physical temperature had to be adjusted to obtain the largest possible bandwidth since the photon energy of the pump-power was not high enough to be uniformly absorbed at low temperatures. The physical temperature was therefore within 1 K below T_c . The reduced gain for sample #B can be explained by the shape of the IV-characteristic (Fig. 5).

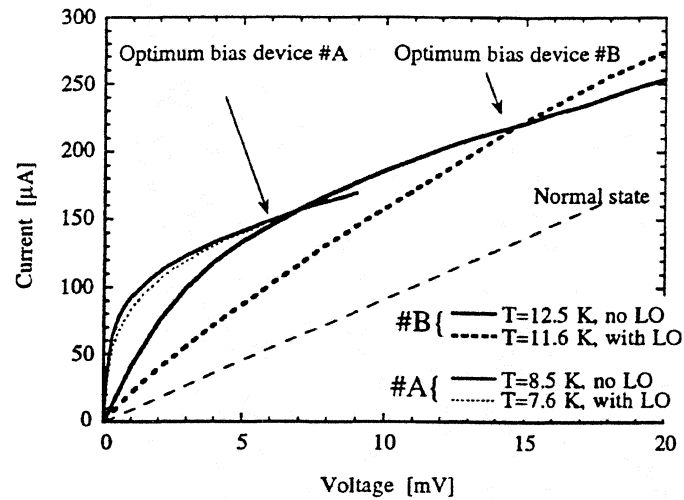


Fig. 5. Pumped and unpumped IV-characteristics for device #A and #B, with optimum bias points for $f_{IF} = 800$ MHz. For device #B the difference between the curves thermally heated and heated by LO is much larger than for device #A.

The difference between the pumped and thermally heated IV-curve is large. The pumped curve for device #B has a smaller differential resistance, which is not much larger than R_0 and gives a smaller self heating parameter C (Eq. 2), and thus smaller gain (Eq. 1). Moreover, film #B, with smaller maximum dR/dT , has a foot structure extending about 1 K below T_c (Fig. 1b), making the transition width even larger. This could be a reason for the degraded IV-characteristic. The value for C which is obtained from R_0 and dR/dT (Fig. 1b and Eq. 6) is larger than one which is obviously not correct as it indicates that there should be a negative differential resistance ($dU/dI < 0$) of the DC IV-characteristic in the bias point. We therefore make the conclusion that neither is the electron temperature given by T_c , i.e. the electrons are not uniformly heated. The quality of NbN film on quartz substrates are worse (e.g. foot structure) than the films made on sapphire or silicon. We expect to obtain improved results with film made on such substrates.

One possible reason for a smaller bandwidth, or increased response at low frequencies for low temperatures (Figs. 3 and 4), when radiation is only absorbed in resistive domains, could be the slow heat redistribution within the domain. At low temperatures the estimated conversion gain is as high as -1 dB. This value for the gain is only valid in the low frequency limit, i.e. for zero IF frequency, and decreases rapidly with frequency. Above a certain frequency the gain at low temperatures will be less than the gain at high temperatures. Thus estimations of conversion gain for $f_{IF} \neq 0$ with Eq. 1 is only possible when the IF response is flat below the IF bandwidth, defined by $f_{max} = (2\pi\tau_{mix})^{-1}$. This is not the case for NbN at low temperatures. For Nb

$f_{\max} \approx 90$ MHz, much less than f_{\max} for NbN, and more or less coincide with the increased response at low frequencies. An estimation of the gain at low temperatures for $f_{IF} \neq 0$ is therefore more correct in the case of Nb films. However, it is predicted that the IF response should always be flat when the signal frequencies $f_s > 2\Delta/h$, i.e. one has uniform heating. Thus there will be a flat response even at the lowest temperature when the signal frequency is large enough.

IMPEDANCE

An attempt has been made to measure the small-signal IF output impedance in the frequency range between 1 MHz and 5 GHz for sample #A at a temperature of about 1 K below T_c (Fig. 6). It was possible to detect a small influence on the HEB from the measurement signal of the network analyser, why this measurement should only be used as a guide of the general behaviour of the output impedance of the HEB. The temperature and bias of the operating point is chosen to give the maximum IF signal at 800 MHz (centre frequency of IF amplifier). In the low frequency limit up to about 100 MHz, the impedance is real and approximately equal to the DC differential

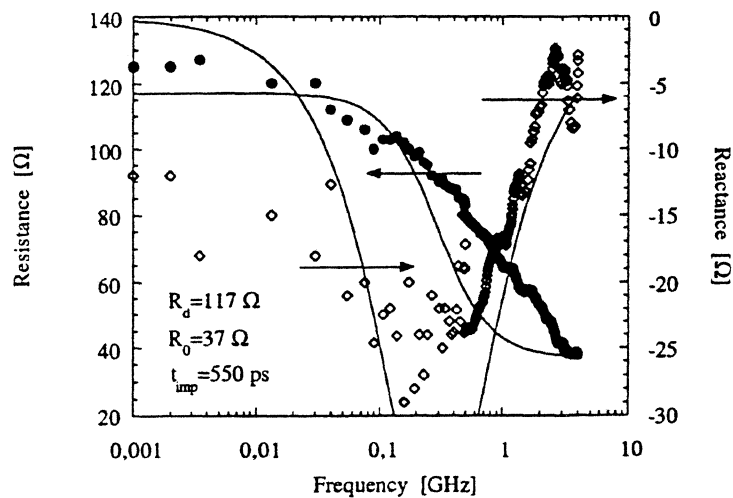


Fig. 6. A rough measurement to show the general behaviour of the resistive and reactive parts of the NbN HEB small signal IF impedance. The measurement was done in the optimum bias point with respect to the conversion gain at 800 MHz IF frequency. The solid lines are fitted curves obtained from Eq. (4). The values used for R_d , R_0 , and τ_{imp} are inserted in the plot.

resistance in the bias point (115 Ω). At 1 GHz the real part of the impedance is about 65 Ω and for frequencies above 3 GHz it equals the DC resistance in the bias point (37 Ω). At about 300 MHz the reactive part of the impedance is maximum and about

-40 Ω . For frequencies above 2 GHz (and below 300 MHz) it is close to zero. A rough estimation of the impedance time constant $\tau_{imp}=550$ ps can be made, taken as an average of the two time constants given by the measured resistive and reactive parts of the impedance, Eq. (4) [15].

$$Z(\omega) = R_d \frac{1 + j\omega\tau_{imp} \frac{R_o}{R_d}}{1 + j\omega\tau_{imp}} \quad (4)$$

where R_d is the DC differential resistance, i.e. $R_d=Z(0)$.

The impedance time constant can as well be derived from the mixing time constant, $\tau_{mix}=240$ ps ($f_{IF}=680$ MHz) as

$$\tau_{imp} \equiv \frac{\tau_{\theta}}{1-C} = \frac{\tau_{mix} \left(1 - C \frac{R_o - R_L}{R_o - R_L}\right)}{1-C} \quad (5)$$

where τ_{θ} is the electron temperature relaxation time.

It is seen that τ_{imp} depends strongly on the self-heating parameter C , which can be obtained in different ways according to

$$C = I_o^2 \frac{dR/d\theta}{V \cdot c_e} \cdot \tau_{\theta} = 0.58 \quad (6)$$

or

$$C = \frac{dU/dI - R_o}{dU/dI + R_o} = 0.59 \quad (7)$$

Eq. 5 gives $\tau_{imp}=640$ ps or 660 ps with C from Eq. (6) and (7) respectively. Considering the large uncertainty in the impedance measurements (the measured time constant for the resistance is three times shorter than the time constant obtained from the reactance, $\tau_{imp,Im}=3 \cdot \tau_{imp,Re}$) the excellent agreement between the measured τ_{imp} and τ_{mix} is probably more or less a coincidence, as the accuracy of the measured τ_{imp} is only within a factor of 3-4. At low temperatures the low frequency impedance increases as the differential resistance increases but we never obtain a measured value larger than 300 Ω , even for a larger differential resistance. This demonstrates that a slow relaxation is important for the low temperature resistive state and contributes even more at frequencies below 1 MHz.

NOISE

The output noise of the mixer as well as the DSB receiver noise has been measured for device #A and #B. The output noise temperature, T_{out} , was measured by comparing the noise levels obtained on a spectrum analyser connected to the IF port of the mixer,

for the device biased in the point for maximum output power, with the noise level in normal state at a temperature well above T_c . Thus

$$\frac{P_{noise,opt}}{P_{noise,normal}} = \frac{T_{out}(1-L) + T_{IF}}{T_J(1-L) + T_{IF}} \quad (8)$$

where T_{IF} is the noise contribution from the room temperature IF amplifier + bias-T etc., T_J is the Johnson noise from the device in normal state working as an ordinary resistor, and

$$L = \left(\frac{R_o - R_d}{R_o + R_d} \right)^2 \quad (8b)$$

is the corresponding mismatch loss, which is the same in normal state and in the bias point since $R_N \approx R_d (\approx 115 \Omega)$ for #A. T_{IF} was measured by comparing the output noise levels for the device in normal state at two temperatures, 77 and 300 K.

The output noise consists mainly of temperature fluctuation noise and Johnson noise, i.e. $T_{out} \approx T_{FL} + T_J$. When the radiation is uniformly absorbed ($\nu > 2\Delta/h$) the electrons have an equivalent temperature $\theta \approx T_c$, and T_J is approximately given by T_c . The temperature fluctuation noise of #A has been measured over the frequency range 20 MHz to 2 GHz at a temperature 7.6 K (about 1 K below T_c) [16], and at 6.8 K. This type of noise has the same output frequency dependence as the IF signal. At 7.6 K it has an equivalent output temperature $T_{FL} \approx 100$ K within the IF band. At the lower temperature 6.8 K, where still $I_c = 0$, there is an overall increase of noise particularly towards lower frequencies (Fig. 7).

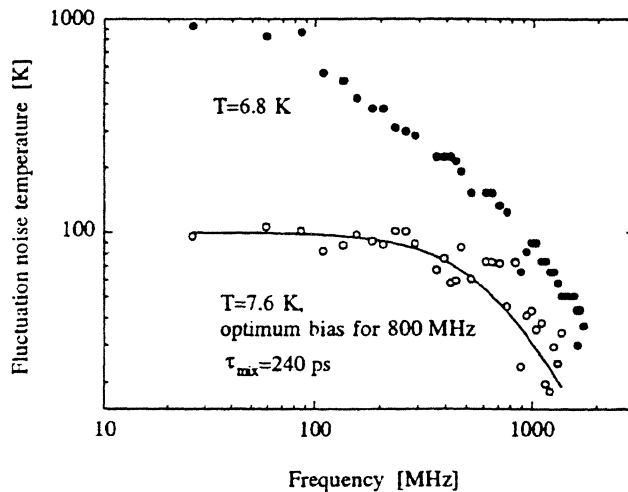


Fig. 7. Output noise temperature due to thermal fluctuation of the electron temperature for sample #A. At 7.6 K this noise shows the same frequency dependence as the IF signal and is about 100 K within the IF band, while for lower temperatures, the noise increases, particularly at lower frequencies.

Fig. 8 gives a general idea of how the output noise is reduced with bias and through heating of the film by different levels of pump power as the film approaches the normal state. The physical temperature is 5 K, well below the temperature when the output noise is flat within the IF-band. From the inset in Fig. 8 it is seen that heating by LO power at this low temperature gives an IV-characteristic with much lower differential resistance than what is obtained by thermal heating of the device. The heating is thus not uniform. We can say very little on the origin of the enhanced noise towards lower temperatures, where we meet a domain contribution, Figs. 7 and 8. It is probably different from the equilibrium thermal fluctuation mechanism and can not be described by the same formulas as the thermal fluctuation noise temperature [17].

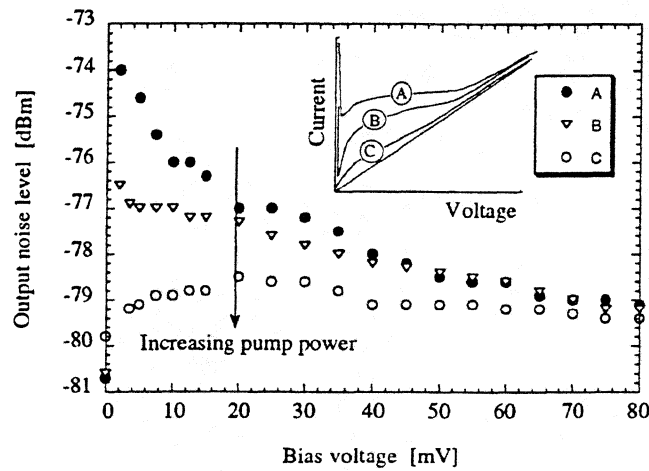


Fig. 8. Output noise level as a function of bias voltage and pump power. The insert shows the IV-characteristics for the different pump levels A, B and C. level A<B<C.

The contribution from $T_{FL}+T_J$ to the double sideband receiver noise temperature within the IF band is given by

$$T_{mix,DSB} = \frac{1}{2G}(T_{FL} + T_J)(1 - L) \approx 200 \text{ K}, \tag{9}$$

where G is the estimated intrinsic conversion gain including IF losses $\approx -6.5 \pm 1$ dB.

Measurements of sample #A with a hot/cold (295/80 K) load facing the input signal port, gave a DSB receiver noise temperature of about 3000 K. These measurements were made within the band of the cooled IF-amplifier (680-920 MHz). This is outside the maximum -3 dB bandwidth of device #A ($f_{IF}=680$ MHz). From Fig. 3 it is seen that in the middle of the amplifier band (800 MHz), and for a physical temperature about 1 K below T_c , the mixer conversion is reduced to about $L_{BW} \approx 4$ dB below the conversion at low frequencies $L_{int} \approx 7$ dB (given by Eq. 1). In Fig. 7 it is seen that also the noise contribution from temperature fluctuations has decreased, from 100 K to about 50 K at

800 MHz. $R(800) \approx 70 \Omega$, thus L is reduced from 0.155 to ≈ 0.05 (Fig.5). From Eq. 9 we then obtain $T_{mix,DSB} = 360 \text{ K}$ at 800 MHz. *Comparing this with the DSB noise temperature obtained from hot/cold measurements, 3000 K, gives that we have an additional loss on the RF side and in the mixer itself of about 8 dB. In TABLE I we have estimated the RF losses to about $L_{RF} \approx 6 \text{ dB}$, about $\frac{3}{2}$ dB below this value.

The noise contribution of the IF chain with the cooled amplifier was again measured using the mixer device as a resistive load. The device is thus heated to its normal state in a temperature range 3-10 degrees above the critical temperature T_c , where the output noise level was measured for several temperatures. No bias current is applied to be sure there will be no noise contribution from the device other than the Johnson noise. The output power had the expected linear dependence on temperature, and gave a noise contribution from the IF chain equal to 12 K.

With sample #B it was possible to measure the mixer noise within the bandwidth of the mixer $f_{max} \approx 1 \text{ GHz}$. The DSB receiver noise temperature was as high as 4700 K but the output noise temperature due to thermal fluctuations was not more than $T_{FL} \approx 50 \text{ K}$. However, as was said previously, the intrinsic conversion gain was much worse for sample #B, -14 dB compared to #A. With $R_d = 100 \Omega$, $T_c = 11 \text{ K}$ we obtain $T_{mix,DSB} \approx 700 \text{ K}$ from Eq. (9). *Comparing this value with $T_{rec,DSB} = 4700 \text{ K}$ obtained from hot/cold measurements, we have an additional loss of about $\frac{3}{7}$ dB on the RF-side.

Notice that an error is introduced in the calculation of the output noise (Eq. 8) for sample #A outside the IF bandwidth and for sample #B, since here R_d is not equal to R_N . Noise data is summarised in TABLE III.

TABLE III

#	R_d [Ω]	R_d^* [Ω]	R_N [Ω]	G [dB]	G^* [dB]	T_{FL} [K]	T_{FL}^* [K]	T_J [K]	$T_{mix,DSB}$			L_{RF} [dB]
									T_{DSB} [K]	T_{DSB}^* [K]	$T_{DSB}^{(1)}$ [K]	
A	115	80	120	7	11	100	50	8.5	200	360	3000	$\frac{3}{8}$
B	-	100	150	-	14	-	50	11	-	700	4700	$\frac{3}{7}$

* At the IF frequency 800 MHz.

(1) Hot/cold measurement, receiver noise temperature

CONCLUSIONS

With heterodyne measurements of NbN HEB devices integrated with double dipole antennas on quartz substrate lenses, we have shown that it is possible to obtain a bandwidth larger than 1 GHz, and a conversion loss about 7 dB. The output noise is

* Including T_{IF} (12K) and

dominated by electron temperature fluctuations, and has an equivalent temperature of about 100 K, with the same frequency dependence as the IF response. Hot/cold measurements gives a DSB receiver noise temperature of about 3000 K. The small signal IF impedance has been measured and we obtained an impedance time constant in good accuracy with the mixing time constant. The measured low and high frequency impedance equals the values obtained from the IV-characteristic. We have seen indication of two different mixing regimes at low temperatures and high temperatures when the signal frequency $\nu > 2\Delta/h$.

The performance of the NbN HEB device can be improved in many ways. The RF coupling losses should be possible to reduce by several dB. NbN films on quartz are of worse quality than films on sapphire or silicon. Thus we expect improved results for NbN devices on the latter substrates, where a sharp superconducting transition (dR/dT is large) can be obtained also for films with higher T_c . More experiments have to be performed to find out if it is possible to obtain both the low output noise of sample #B with the better conversion of sample #A. Further improvement is also expected for signal frequencies $\nu > 2\Delta/h$.

ACKNOWLEDGEMENT

We are greatly thankful to B. Voronov and V. Siomash for manufacturing of NbN films. This work was supported by the Swedish National Board of Industrial and Technical Development (NUTEK), and by the Russian Council on High-Tc Problems under Grant no. 93169. The research was made possible in part by Grant no. NAF000 from the International Science Foundation.

REFERENCES

- [1] T. W. Crowe, R. J. Mattauch, H. R. Röser, W. L. Bishop, W. C. B. Peatman, and X. Liu, "GaAs Schottky Diodes for THz Mixing Applications," *Proc. IEEE*, vol. 80, pp. 1827-1841, 1992.
- [2] E. R. Brown, J. Keene, and T. G. Phillips, "A Heterodyne Receiver for the Submillimeter Wavelength Region Based on Cyclotron Resonance in InSb at Low Temperatures," *Int. J. Infrared Millimeter Waves*, vol. 6, pp. 1121-1138, 1985.
- [3] M. J. Wengler, "Submillimeter-Wave Detection with Superconducting Tunnel Diodes," *Proc. IEEE*, vol. 80, pp. 1810-1826, 1992.
- [4] J. X. Yang, F. Agahi, D. Dai, C. F. Musante, W. Grammer, K. M. Lau, and K. S. Yngvesson, "Wide-bandwidth electron bolometric mixers: a 2DEG prototype and potential for low-noise THz receivers," *IEEE Trans. Microwave Theory Tech.*, vol. 41, pp. 581-589, 1993.
- [5] E. M. Gershenson, G. N. Gol'tsman, I. G. Gogidze, A. I. Elant'ev, B. S. Karasik, and A. D. Semenov, "Millimeter and submillimeter range mixer based on electronic heating of superconducting films in the resistive state," *Sov. Phys. Superconductivity*, vol. 3, pp. 1582-1597, 1990.
- [6] H. Ekström, B. Karasik, E. Kollberg, and S. K. Yngvesson, "Conversion Gain and Noise of Nb Superconducting Hot Electron Mixers," *IEEE Trans. Microwave Theory Tech.*, vol. 43, 1995. (in press)

- [7] A. Skalare, W. R. McGrath, B. Bumble, H. G. LeDuc, P. J. Burke, A. A. Verheijen, and D. E. Prober, "A Heterodyne Receiver at 533 GHz using a Diffusion-Cooled Superconducting Hot Electron Bolometer Mixer," *IEEE Trans. Appl. Superconductivity*, vol. 5, 1995. (in press)
- [8] D. E. Prober, "Superconducting terahertz mixer using a transition-edge microbolometer," *Appl. Phys. Lett.*, vol. 62, pp. 2119-2121, 1993.
- [9] A. Skalare, H. van de Stadt, T. de Grau, R. A. Panhuyzen, and M. M. T. M. Dierich, "Double dipole antenna SIS receivers at 100 and 400 GHz," presented at 3rd Int. Symp. on Space THz Technology, 1992.
- [10] D. F. Filipovic, S. S. Gearhart, and G. M. Rebeiz, "Double-slot antennas on extended hemispherical and elliptical silicon dielectric lenses," *IEEE Trans. Microwave Theory Tech.*, vol. 41, pp. 1738-1749, 1993.
- [11] B. M. Voronov, G.N.Gol'tsman, E. M. Gershenson, L. A. Seidman, T. O. Gubkina, and V. D. Siomash, "Superconducting properties of ultrathin NbN films on different substrates," *Superconductivity: Physics, Chemistry, Engineering*, vol. 7, pp. 1097-1102, 1994. (in Russian)
- [12] A. F. Andreev, *Sov. Phys. JETP*, vol. 19, pp. 1228, 1964.
- [13] F. Arams, C. Allen, B. Peyton, and E. Sard, "Millimeter Mixing and Detection in Bulk InSb," *Proc. IEEE*, vol. 54, pp. 308-318, 1966.
- [14] Y. P. Gousev, G.N. Gol'tsman, A. D. Semenov, E. M. Gershenson, R. S. Nebosis, M. A. Heusinger, and K. F. Renk, "Broadband ultrafast superconducting NbN detector for electromagnetic radiation," *J. Appl. Phys.*, vol. 75, pp. 3695-3697, 1994.
- [15] A. I. Elant'ev and B. S. Karasik, "Effect of high frequency current on Nb superconducting film in the resistive state," *Sov. J. Low Temp. Phys.*, vol. 15, pp. 369-383, 1989.
- [16] H. Ekström and B. Karasik, "Electron Temperature Fluctuation Noise in Hot-Electron Superconducting Mixers," *Appl. Phys. Lett.*, accepted.
- [17] B. S. Karasik and A. I. Elantev, "Analysis of the Noise Performance of a Hot-Electron Superconducting Bolometer Mixer," presented at 6th Symp. on Space Terahertz Tech., Pasadena, USA, 1995.